ASH FUSION TEMPERATURES AND THE TRANSFORMATIONS OF COAL ASH PARTICLES TO SLAG

S. Gupta, T.F.Wall, R.A.Creelman and R.Gupta
Department of Chemical Engineering
University of Newcastle, Callaghan, NSW 2308, Australia

Keywords: Ash fusion, viscosity and shrinkage.

ABSTRACT

A mechanistic study is detailed in which coal ash is heated with its shrinkage measured continuously up to a temperature of 1600°C. The temperatures corresponding to the rapid rate of shrinkage are shown to correspond to the formation of eutectics identified on phase diagrams. Samples were therefore heated to these temperatures, cooled rapidly and examined with an SEM to identify the associated chemical and physical changes. The progressive changes in the range of chemical analysis (from SEM), the extent of undissolved ash particles and porosity were then quantified and related to homogenisation, viscosity and ash fusion mechanisms.

INTRODUCTION

Ash deposition on furnace walls in pf (pulverised fired) furnaces is called slagging when it occurs in the high temperature areas of furnaces directly exposed to flame radiation and fouling in other regions such as tubes in the convection section of the boiler. The characterisation of coal ash for its tendency to slag and foul has been traditionally related to the bulk chemistry of the ash and ash fusion temperatures. There are well-documented shortcomings of these approaches relating to their uncertainties as predictive tools for plant performance, that is, poor repeatability and reproducibility of ash fusion measurements. Of particular concern is the estimation of the initial deformation temperature (IDT). IDT is the temperature at which the rounding of the tip of an ash cone is noted, which has been accepted as the temperature where the ash first softens and therefore becomes sticky. The nature of physical and chemical changes occurring during melting of coal ash has been investigated in the current study to provide an alternative procedure to the ash fusion test. The characteristic melting temperatures then are related to the transformations, and reactions of ash and these are interpreted in terms of their importance to fouling and slagging in furnaces.

EXPERIMENTAL

The current study is based on a range of samples selected from domestic power stations to those exported from Australia as steaming coals. Several export coals were selected on the basis of difficulty of the estimation of their IDT's. Laboratory ash was prepared for all the samples and ashes from some of the corresponding power stations were also obtained. Different laboratories reported a wide variation in IDT estimation, the difference being as great as 400°C in some cases.

Several techniques have been tried to investigate the fusibility of bituminous ashes in a related study as detailed elsewhere (Wall et al., 1995). The major events observed in these techniques are illustrated in Figure1. The top two plots in Figure1 are based on the HRL Test (Ellis, 1989). The electrical resistance and shrinkage of compacted ash pellets are recorded concurrently from room temperature to about 1350°C in this test. The third plot indicates the shrinkage of compacted ash pellets sandwiched between two tiles as developed at ACIRL (Coin, et al. 1995). The last plot is based on the TMA (thermomechanical analysis) technique developed by the CSIRO Division of Coal and Energy Technology. The current paper will be restricted to results obtained from the last technique.

TMA Technique (Thermomechanical Analysis)

Shrinkage measurements are frequently used in metallurgy and ceramic science to study the physical properties at high temperatures. Raask(1979), Ellis(1989), Lee(1991), Gibson(1991) and Sanyal(1993) have studied electrical resistance and shrinkage properties for sintering and fusion characteristics of ashes in the past. However, a systematic study comprising several types of measurements, laboratory ash and combustion ash with investigations of fusion mechanisms for temperatures up to 1600°C has been lacking. TMA technique involves measurements of the shrinkage of loose ash(~35mg.) in a specially designed sample holder which is located between a cylindrical graphite container with a flat bottom and a rod with a tapered end. As the assembly (ash) is heated from room temperature to 1600°C, the rod sinks into the ash and when eventually flows as slag into the annular gap between the rod and the container. The samples were heated in neutral environment as per AS (Australian Standards) requirements. The output of this experiment provides 3 to 4 'peaks' (maximum rate of shrinkage with temperature) of different intensity and at different temperatures which are related to melting characteristics of the sample as shown in Figure1. There is no significant shrinkage in most of the samples below 900°C. The temperatures associated with particular shrinkage levels were noted as T(x%).

Studies to Identify Transformations

Compacted ash pellets were heated under standard AS reducing conditions and rapidly quenched in air to freeze the samples. The chemical composition of liquid phases and slags were determined from sectioned samples of these pellets using a scanning electron microscope (SEM) and electron dispersive spectrum (EDS). Micrographs of the samples were also obtained to compare the porosity and extent of undissolved particles. Bulk density of some of the samples has also been measured at different temperatures.

RESULTS

Mechanism of Ash Fusion

The current observations are based on twenty nine samples. Most of the samples can be grouped into four categories, and represented by particular samples as follows: i) ash with a high SiO_2/Al_2O_3 ratio, low Fe_2O_3 and poor reproducibility for the IDT e.g. EN3; ii)ash with a SiO_2/Al_2O_3 ratio within the norm of Australian coals, low Fe_2O_3, and very poor reproducibility for the IDT e.g. EN6; iii) ash with high Fe_2O_3(11%) e.g. EQ1with good reproducibility and iv) and ash with high CaO(16%), e.g. ET2 with good

reproducibility for the IDT. TMA measurements provided 'peaks' identifying rapid fusion events during heating. These 'peaks' have been related to formation of eutectics identified on appropriate phase diagrams (Wall, et al., 1995). Shrinkage results demonstrated occurrence of the peaks in three distinct groups. Lower temperature peaks up to 1100°C were related to eutectics in SiO_2 - Al_2O_3 - K_2O system and 1200°C peaks to SiO_2 - Al_2O_3 - FeO system. Peaks in the range 1220°C to 1440°C have been correlated to FeO and CaO reactions with various proportions of SiO_2 and Al_2O_3.

Homogeneity and Porosity of Samples:

The melt composition will change continuously with temperature till ash is transformed completely to a homogeneous liquid. The chemical composition of slag should then be of the bulk ash. The melt composition was determined for at least 10 points per sample at one temperature using SEM and EDS mode. Major variation in the melt composition is due to different extent of dissolution of silica particles. SiO_2(wt.%) concentration in the melt has been selected to illustrate the homogenisation of liquid phase. SiO_2 in melt reaches to bulk ash composition rapidly in high iron sample EQ1 as shown in Figure2, where the EN3 and EN6 melt approach to the bulk ash composition at a higher temperature.

Ternary diagrams have also been used for describing the change in melt composition. The chemical composition from point analysis was normalised to three component system i.e. SiO_2 -Al_2O_3 - CaO for ET2 and SiO_2 -Al_2O_3 - FeO for other samples. The normalised analyses of EN6, EQ1 and ET2 are presented on ternary diagrams of SiO_2 - Al_2O_3 - FeO and SiO_2 - Al_2O_3 - CaO as shown in Figure3. EQ1 and ET2 melt composition range narrows to that of bulk ash at lower temperatures as compared to EN6(Figure3). CaO appears to be most important constituent for rapid homogenisation at various stages.

At low temperatures diffusion rates are slow therefore melt formation proceeds slowly. As the ash is heated open pore network transforms to micropores and a minimum porosity. Melting and reaction occurs to form the first liquid phase that has a composition close to iron cordierite. This liquid may start flowing to fill the open network and hence contribute to initial densification. The reaction of this melt phase with specific solids (SiO_2 rich) until progressive depletion of the solids occurs and finally slumping of the pellets as the proportion of the liquid increases significantly. Air entrapped in the sample causes pore formation. It was observed that pore formation increases with iron content. Most of the porosity is either closed or in the form of spherical pores. Majority of the samples indicate that T(50%) (temperature corresponding to 50% shrinkage) is associated with closed and spherical pore structure. Gibson(1991) also observed similar trends. Bulk porosity keeps on decreasing till formation of closed pores takes place. Closed porosity is found to be increasing rapidly after T(50%) in most of the cases. The bulk density estimated from pellet dimensions also indicated that high alkali samples acquire minimum porosity at lower temperatures compared to high silica samples. It was also observed that temperatures corresponding to minimum porosity lie between 1200° to 1300°C. Physical changes before 50% shrinkage may depend on the permeability of liquid through the open porosity. After 50% shrinkage, the rate of shrinkage may depend on the rate of dissolution of residual silica in the melt (i.e. amount and particle size of quartz in the initial sample). Image analysis of electronmicrographs of various samples indicated less than 25% undissolved particles at T(50%).

AFT and Alternative Shrinkage Temperatures

The traditional AFT test involves observation of four temperatures (IDT, ST, HT and FT) depending on the physical state of the ash cone. Huffman(1981) observed that at IDT most of the melting is completed and it was also estimated that glass phase was more than 75%. Figure5 shows the linear shrinkage associated with IDT and some 'peak' temperatures. The first peak, i.e. first important fusion event in majority of the samples was observed around ~10% shrinkage of ash. The second peak occurred at <30% shrinkage of most of the samples, except for high iron and high CaO, which are associated with ~50% shrinkage at the second important event. It can be seen that IDT is associated with approximately ~50% shrinkage for EQ1 and ET2 samples of good reproducibility and around 60% for poor reproducibility samples e.g. EN3 and EN6 (Figure 4). The IDT clearly does not represent first shrinkage event.

The temperatures corresponding to these fusion events may be used for ash deposition characterisation. Figure 5 illustrates a ranking criteria for ash deposition based on temperature vs shrinkage plot for many samples. The samples requiring higher temperatures for a given shrinkage level are expected to be associated with least deposition, while those at the bottom are expected to be most troublesome. Hence ET2 (high CaO) would provide worst deposition, whereas PQ2(least alkali) should provide least deposition. However, the location of a particular sample within this ranking will depend on the temperature in different regions of the plant. In practical terms, this implies that ranking will depend on the temperature in different parts of the plant.

Correlation of shrinkage with ash viscosity, and sticky particles

The current understanding of the of the ash deposition is based on the stickiness of the particles. If the particles are sticky they will adhere to a surface on impact. Many studies have related stickiness to the viscosity of the particles which, in turn, has been calculated from the chemical composition. The viscosity calculated from the known composition of the ash samples therefore provides a basis for estimating theoretical temperatures for particles to be sticky, which can be related to the extent of shrinkage measured at these temperatures. Boni et al. (1990) suggested that ash particles with viscosity $>10^7$ Pas are not sticky and will not collect on the heat transfer surface. The sintering and slagging has also been related to viscosity of ash particles by Raask (1985). Figure 6 indicates the range of viscosity of the liquid slag generated from the ash samples which is calculated from the Urbain correlation (Urbain et al., 1981) based on the ash chemistry. This figure also provides the shrinkage range of importance to ash deposition. All ash samples fall within the viscosity range of 10^5 to 10^7 Pas at 25% shrinkage (Figure 7). Therefor it may be suggested that this shrinkage level is appropriate as criterion for ash stickiness. Examination of electronmicrographs from quenched samples also indicate the significant proportion of liquid phase

corresponding to these temperatures. It can be seen from this figure that ash particle impinging onto walls will be sticky at a similar temperature at which liquid formation has been observed in the pellets.

CONCLUSIONS

1. IDT clearly does not represent the first fusion event.
2. T(25%) is found to be associated with significant particle deformation.
3. T(50%) is related to formation of closed or spherical pores, which corresponds to >75% melt phase.
4. The temperatures corresponding to particular shrinkage events may be used as alternate ash fusion temperatures.

ACKNOWLEDGMENTS

We are most grateful to Mr. Dick Sanders of Quality Coal Consulting Pty. Ltd. for managing the project, selecting samples and providing insights into the AFT procedures. The study was supported by the Australian Coal Association Research Program with Mr. Grant Quinn of BHP Australia Coal as project monitor. The assistance of Dr. John Saxby at CSIRO is greatly appreciated.

REFERENCES

Boni et al. (1990), Transformations of Inorganic Coal Constituents in Combustion System, DOE Report No. AC22 - 86PC 90751, March (1990).

Coin, C., Reifenstein, A.P. and Kahraman H. (1995), Improved Ash Fusion Test, Engineering Foundation Conference on Application of Advanced Technologies to Ash - related Problems in Boilers, USA.

Ellis, G.C. (1989), The Thermomechanical, Electrical Conductance and Chemical Characteristics of Coal Ash Deposits, NERDDP Project No. 1181 Final Report Volume III, SECV R & D Dept, Australia.

Gibson, J.R. and Livingston, W.R. (1991), The Sintering and Fusion of Bituminous Coal Ashes, Engineering Foundation Conference on Inorganic Transformations and Ash Deposition During Combustion, Palm Coast, Florida.

Huffman, P.G., Huggins F.E. and Dunmyre G.R. (1981), Investigation of the High Temperature Behaviour of Coal Ash in Reducing and Oxidising Atmospheres, Fuel, 60, 585-597.

Lee, G.K. et al. (1991), Assessment of Ash Sintering Potential by Conductance and Dilatometry, Pittsburgh Coal Conference.

Raask, E. (1979), Sintering Characteristics of Coal Ashes by Simultaneous Dilatometry - Electrical Conductance Measurements, J. Thermal Analysis 16, 91.

Raask, E. (1985), Mineral Impurities in Coal Combustion. Hemisphere Publishing Corporation USA.

Sanyal, A. and Mehta, A.K. (1994), Development of an Electrical Resistance Based Ash Fusion Test. The Impact of Ash Deposition in Coal Fired Furnaces, p445-460, Taylor and Francis, Washington.

Urbain G. et al. (1981), Trans. J. Br. Ceram. Soc., Vol. 80, p139-141.

Wall, T.F. et al. (1995), Coal Ash Fusion Temperatures - New characterisation Techniques, and Associations with Phase Equilibria, Engineering Foundation Conference on Application of Advanced Technology to Ash - Related Problems in Boilers, New Hampshire, USA.

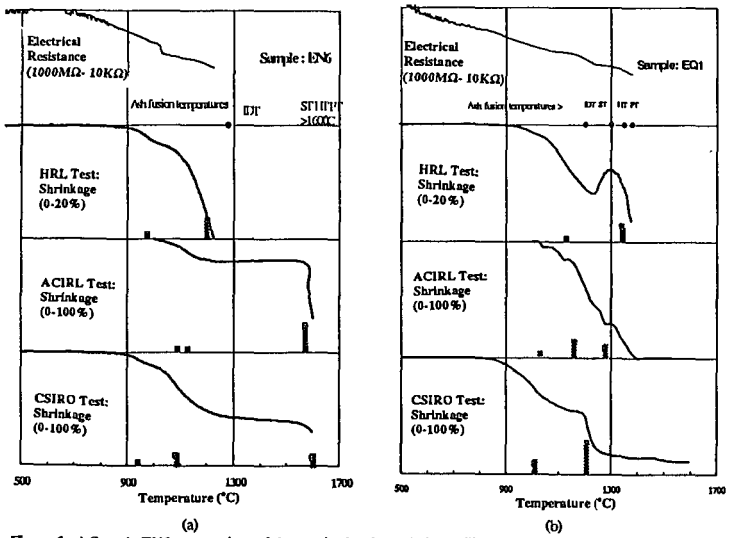

Figure 1. a) Sample EN6, comparison of the results for the techniques. Top plot - electrical resistance data from HRL test, bottom of three plots - shrinkage experiments reported as progressive ash sample linear dimension on heating. The bars indicate 'peak' temperatures of rapid change in ash sample heating, b) Sample EQ1.

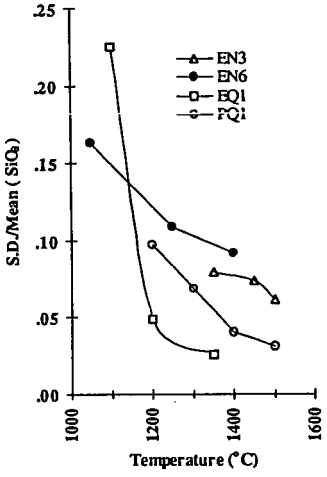

Figure 2. Variation in SiO_2 composition in melt phase, for different samples expressed as the standard deviation normalised to the mean.

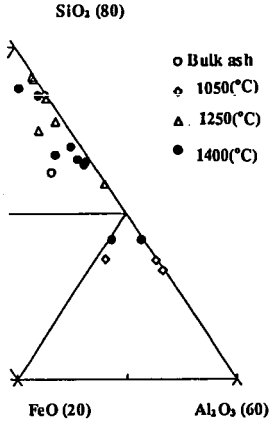

Figure. 3(a)

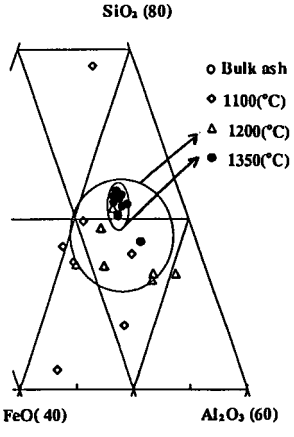

Figure 3(b)

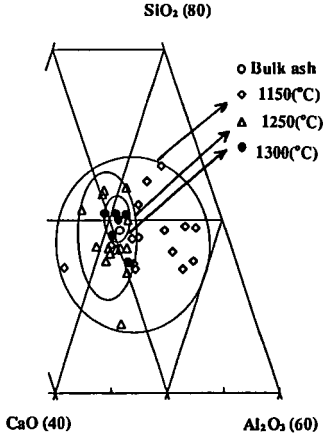

Figure 3(c)

Figure 3. Ternary plot for melt compositions for a) EN6, b)EQ1 and ET2.

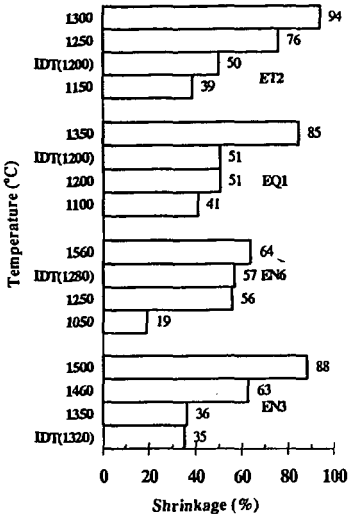

Figure 4. Shrinkage(%) at peak temperatures and IDT for samples EN3,EN6,EQ1 and ET2.

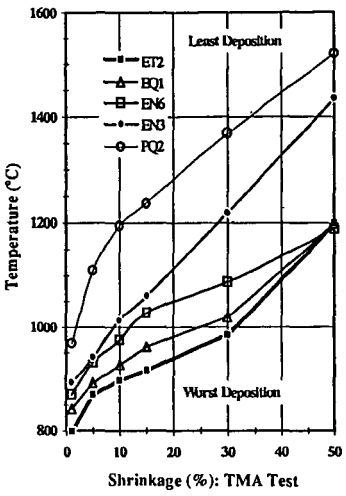

Figure 5. Relative sample ranking plot for ash deposition based on shrinkage(%) temperatures.

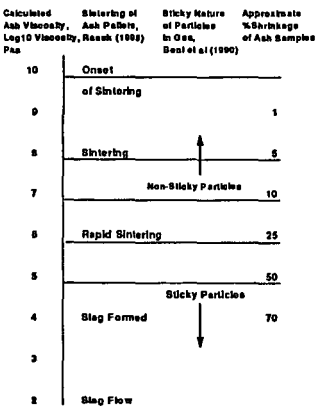

Figure 6. Association between physical state of ash, sintering and sticky nature of particles in the furnace.

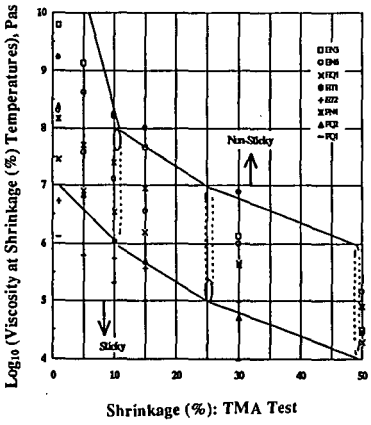

Figure 7. Correlation of calculated viscosity (Urbain' Model) and different levels of shrinkage with regions for sticky and nonsticky particles.